Unified Design Method for Flexure and Debonding in FRP Retrofitted RC Beams

G.X. Guan, Ph.D.[1]; and C.J. Burgoyne[2]

Abstract

Flexural retrofitting of reinforced concrete (RC) beams using fibre reinforced polymer (FRP) plate is a common way to increase the flexural capacity. There is a lack of rational design method to determine where the strengthening plate can safely be curtailed. As a result, retrofitted beams commonly fail by debonding of the FRP plate, which occurs well before the target flexural capacity. Debonding is brittle failure and thus ductility of the retrofitted beam needs to be ensured by debonding prevention. With sufficient ductility the ultimate strength can continuously increase beyond steel yields with the elastic behaviour of the FRP strengthening plate. Debonding prevention has been accounted-for empirically in most design approaches so far.

The Global Energy Balance Approach (GEBA) using fracture mechanics has been proposed to determine the debonding load of an FRP-RC beam that is affected by the plate curtailment location. The GEBA results for various FRP-RC beams can be summarised using debonding contours on plots of moment capacity against the safe plate curtailment locations, and the debonding contours constructed in this way for the beams with the same ratio of depth to fracture energy are virtually the same. This paper shows how GEBA can be incorporated into the design process to prevent premature debonding of the FRP plate. The method makes use of the debonding contours and derives from these simplified design charts that could be made available to designers. The retrofitting design consideration and the theoretical background of this unified design method are first explained, followed by the derivation of the conceptual design charts. Numerically correct design charts are then constructed for a wide range of

Introduction

FRP plate retrofitting considerations

FRP plates can be used to enhance the capacity of under-reinforced RC beams but has the effect of reducing ductility. It is relatively easy to decide how much FRP is needed to achieve a certain strength, but it is harder to ensure sufficient ductility and retrofitted beams are known to suffer from premature debonding at loads below their design strength. This paper shows how to design beams for strength, ductility and debonding prevention.

Figure 1 shows typical load deflection relationships for three beams. Curve (A) applies to an unstrengthened under-reinforced beam; it has a relatively long plateau at virtually constant load as the steel yields before the concrete crushes. Curve (B) shows the effect of adding a moderate amount of strengthening; the beam yields at a higher load because of the presence of the CFRP, and continues to resist more load after the steel yields because the CFRP remains elastic. However, final crushing of the concrete occurs at a lower deflection because the neutral axis is deeper. The limiting case is shown in Curve (C) for a balanced section, where the concrete crushes at the same time as the steel yields.

The original service load is shown as $P_{u\text{-}s}$ while the original ultimate load capacity is $P_{u\text{-}u}$. There are several limits on the amount of flexural strengthening.

1. In order to prevent brittle failure, most RC beams are under-reinforced. Thus a beam should not be over strengthened to become over-reinforced, so the corresponding balanced section design limits the amount of FRP to be added (Curve C).
2. It is undesirable for the beam to undergo plastic deformation under normal service loads to avoid accumulation of plastic deformation, so the retrofitted service load limit ($P_{s\text{-}y}$) is calculated from the moment that causes first yield of the original steel

a place where the flexural strains are small. Strain criteria are thus not relevant. A study based on fracture analysis of concrete, which relates the change in the strain energy in the beam and the potential energy of the load to the energy that is released in the concrete when the fracture propagates has been used to predict when debonding would occur. This is known as the Global Energy Balance Approach (GEBA) (Achintha and Burgoyne 2008; Gunes et al. 2009; Carpinteri et al. 2009; Guan (2012); Guan and Burgoyne 2012). The key comparison is between the Energy Release Rate G_R with the Fracture Energy of Concrete G_f. The energy release rate is calculated by comparing the energy difference per unit area for the same beam under both presumed debonded and intact states with moment-curvature models for beam energy estimate. The particular value that should be chosen for G_f will be discussed later but is normally within the range 0.05 to 0.3 N/mm (Shah and Carpinteri 1991; Bazant and Becq-Giraudon 2002).

A parametric study of GEBA has been presented by the authors in Guan (2012), where it is shown that a debonding contour (DBC) plot can be used as the PE debonding criterion: G_R varies as a function of the loading state at which debonding occurs and as a function of where the fracture takes place. G_R is determined from M-κ models and the DBC can be plotted on a graph of normalised moment capacity ($M/(f_c'bd^2)$) against curtailment location (L_{cur}/L_{shear}), which allows the strength design and the debonding design to be combined, as shown in Fig. 2.

The DBC is where the G_R surface intercepts the horizontal plane that is defined by G_f. The DBC varies for beams with different depths, reinforcing steel, FRP material etc. A detailed discussion of the DBC is found in Guan (2012) where it was shown that a normalised

defines a limiting maximum curtailment length. If a beam is designed such that the beam state point lies above this dashed line, premature debonding occurs before the beam's flexural capacity is reached.

It is axiomatic that the unstrengthened beam was under-reinforced, so debonding prevention is going to depend heavily on the tension steel ratio (ρ_s) as well as the FRP ratio (ρ_f). To strengthen a particular RC beam, ρ_s is fixed but the designer can change ρ_f, whereas when considering the design of new beams ρ_s also varies. The effect of these two changes are shown separately in Figs 4 (a) and (b); adding either type of reinforcement always moves YL to the right (YL1 to YL2), but it has different effects on the DBC. Increasing ρ_f means that debonding occurs more easily so the debonding line moves upwards. In contrast, with a larger ρ_s, debonding is less likely so the debonding contour moves downwards. The maximum curtailment ($L_{cur\text{-}max}$) changes correspondingly.

In order to make the above design charts cover a wide range of design cases, say for the practical range for ρ_s from 0.4 to 2.0% and ρ_f from 0.1 to 1.5%, a very large number of DBCs and YLs would be needed and the charts would be very complicated. However, it is noted that the critical point is the intersection point of the DBC and YL. Any designed beam state point below and to the left of this point is safe, which leads to the simpler design charts described below. Two charts will be constructed; one for the pre-yielding stage which will be shown to depend on the amount of steel, and the other will cover the post-yield condition and will depend on the amount of FRP plate.

Although the service load must occur while the steel is still elastic, it has been noted above that the beams may have to carry loads above yield in order to provide sufficient reserve of strength. It is essential that the FRP does not debond before the ultimate strength of the beam is reached. This can be accomplished by means of a different set of curves, which are constructed in the same way as the STI curves, this time varying $°_f$ only. The result is the *FRP-ratio track of intercepts* (FTI) (Fig.6(a)).

As with the STI curves, one FTI curve replaces multiple DBCs. For any particular design, the FTI line always lies below the DBC line once the applied moment exceeds the yield moment (Fig 6(b)). Thus, using the FTI line to determine where the plate should be curtailed is conservative for the post-yield condition. If the reserve of strength that is required beyond yield is high, it is possible that a negative curtailment is predicted as shown in Fig.6(b) (no positive intercept for the FTI at $1.5M_y$). This indicates that an anchor is required in addition to the bond.

Since increasing $°_s$ makes debonding less likely while an increase of $°_f$ makes it more likely, the FTI and STI curves have a similar trend but different inclinations and for a particular combination of ($°_s$, $°_f$) they cross each other at the yielding state.

Unified design procedures

It is now possible to produce a unified design procedure, making use of the STI and FTI curves.

1. It is assumed that an existing beam is being strengthened, so the area of steel is known, fixing $°_s$.

The charts given below are constructed for beams with cylindrical concrete strength f_c' = 37 MPa, with steel yield strength f_y = 530 MPa and Young's modulus E_s = 200 GPa, and with FRP elastic modulus E_f = 165 GPa. The STI and FTI are the locus of intersections of YLs and DBCs. Here the YLs are constructed assuming the tension steel yields at the strain f_y/E_s, the FRP plate behaves elastically, and the concrete in compression follows an unfactored Hognestad-type parabolic stress-strain relationship (Hognestad et al. 1955). When considering DBC, the most important parameter is the ratio h/G_f (MPa^{-1}). It was shown in Guan (2012) that DBCs for beams with the same h/G_f value are virtually identical. Thus the DBCs and the resulting STI and FTI charts below apply to all the beams having the same h/G_f.

Construction of detailed STI design charts

The STI curves can give a conservative design curtailment in the pre-yielding stage, so that they are used to consider debonding prevention for the service state. Fig. 8(a) shows the construction of a typical STI design chart that relates to a 400 mm deep beam, with G_f taken as 0.15 N/mm, so $h/G_f = 2.67\times10^3$ MPa^{-1}. It has been produced by keeping $°_f$ constant (at 0.5%) and varying $°_s$ continuously. The family of thin curved lines are the DBCs for different values of $°_s$, while the different vertical dashed lines are the corresponding YL lines. The darker curved line is the STI which goes through the intersections of the corresponding pairs of DBCs and YLs. The darker solid (vertical) line relates to ρ_s = 1.0%. One STI curve covers the retrofitted design of a beam with a certain depth and $°_f$ value, but various $°_s$ values. A similar set of curves is shown in Fig 8(b) for a beam of depth 800 mm and fracture energy 0.15 N/mm, so $h/G_f = 5.3\times10^3$ MPa^{-1}

Construction of detailed FTI design charts

The FTI curves can be constructed in a similar way. They give a conservative design curtailment in the post-yielding stage and are thus adopted to ensure that debonding does not occur up to the ultimate capacity. They are by keeping ε_s constant and varying ε_f continuously. Figure 11(a) relates to a beam of 400 mm deep, with G_f taken as 0.15 N/mm; a similar set of curves is shown in Fig 11(b) for a beam with depth of 800 mm.

By repeating the process for different ε_s, a family of FTI is given to cover all the design cases for 400 mm deep beams with h/G_f value as 2.67×10^3 MPa^{-1} (Fig 12).

As with the STI Band figures, the FTI Band figures are used to consider designs for beams with the same h/G_f value but different depths. The FTI Band chart for $h/G_f = 2.67\times10^3$ MPa^{-1} is as shown in Fig. 13, where the 1000 and 200 mm depth gives the left and right boundaries respectively. The design procedure using FTI Band figures is the same as using STI Band figures.

Significance of the simplified design

A pair of STI and FTI Band charts is required for one design to consider both service state and ultimate state. Since h/G_f typically has a value in the range $0.5 – 20\times10^3$ MPa^{-1} for beams ranging from 200 to 1000 mm deep, and having a G_f ranging from 0.05 to 0.30 N/mm, in total, about ten pairs of STI and FTI Band charts are able to cover most design scenarios. Thus, the simplified design with STI and FTI Band charts provides a convenient way for practical engineering.

determines which sets of design charts to use is h/G_f , which is 400/0.15 = 2.67 MPa^{-1} in this case. Fig. 16(a) is a reproduction of Fig. 10, but with the relevant lines highlighted. For the service state, a vertical line is first drawn at $M/(f_c'bd^2)$= 0.176 which represents the moment capacity required at service after retrofitting. Second, the maximum curtailments for beams with depths of 200 mm and 1000 mm are given by its intersections with the STI curves at ρ_f = 0.7%, as L_{cur}/L_{shear} = 19.5% and 22.5% respectively. Then the maximum curtailment for the 400 mm beam in the problem is obtained from linear interpolation as L_{cur}/L_{shear} = 20.3%.

When considering the ultimate state, the FTI band charts are used for debonding prevention; Figure 16(b) is a reproduction of Fig. 13, again with the relevant lines highlighted. Following the same procedures, the maximum curtailment for the beam is estimated as L_{cur}/L_{shear} = 16.0%. Consequently, the ultimate state governs the debonding prevention, and the FRP plate should be curtailed less than 16.0% of the shear span away from the supports.

As explained in Sections 2 & 3 above, the curtailments predicted from the STI and FTI band charts are conservative. The exact maximum curtailment obtained from DBC charts (exact design) is also provided here (Fig. 17). The maximum values of L_{cur}/L_{shear} given by the exact design at service and ultimate states are 24.8% (intercepting $M_{s\text{-}s}$) and 16.8% (intercepting $1.5M_{s\text{-}s}$) respectively, which are greater than those predicted by simplified design above. Furthermore, if the FRP plate is curtailed at 17.8% of the shear span, it debonds when the tension steel yields. If the FPR plate is curtailed to 16.8%, debonding and crushing of compressive concrete almost occur simultaneously, since in this case $M_{u\text{-}s}$ (= 0.266) is close to $M_{s\text{-}s}$ (= 0.264). These values all exceed the value of 16.0% given by the simplified design charts. It should be noted that the DBC curves would not generally be available to designers, whereas it is suggested that simplified STI and FTI band charts could be provided.

This new method provides a way of incorporating a fracture mechanics approach to debonding in a conventional beam design.

APPENDIX. Flexural capacity design for the beam in the worked example

STEP 1 Assessment of original capacity

The original design flexural capacity corresponds to the first yield of the section, as shown in Fig. 18.

The concrete compression is calculated using an equivalent rectangular stress distribution according to ACI318-08, where α_1 and β_1 are taken as 0.85 and 0.77 respectively, and the results are in Fig. 18(b). From force equilibrium:

$$0.85 \times 0.77 \times f_c' bx + \circ_{sp} bdE_s £_{sp} = \circ_s bdf_y \qquad (1)$$

where $£_s = f_y / E_s = 0.00265$ and $£_{sp} = \dfrac{x - d_p}{d - x} £_s$

Substituting values and solving gives:

x = 77.5 mm; F_{cc} = 563.2 kN; F_{sc} = 17.2 kN; F_{st} = 580.4 kN.

Since the beam is under-reinforced, the contribution of the nominal compression steel is negligible. The moment capacity of this unstrengthened section (at yield) is thus:

$$M_{u-u} = M_{u-y} = F_{st}(d - 0.5 \times 0.77x) = 580.4 \times (365 - 0.5 \times 0.77 \times 77.5) = 194.5kNm \qquad (2)$$

STEP 2 Design of amount of strengthening

The beam is now to be strengthened so that $M_{s\text{-}s}$ = 259.4 kNm, and $M_{s\text{-}u} > 1.5\ M_{s\text{-}s}$ so is 389.1 kNm. After some trial and error it is found that FRP plate having a cross-sectional area equal to 0.7% of the beam section *(ρ_f = 0.7%)* will provide the necessary strengthening. This amount of FRP is sufficient, by checking the new service and ultimate conditions, as shown in Fig. 19.

$P_{s\text{-}s}$, $P_{s\text{-}y}$, $P_{s\text{-}u}$ -- strengthened service/yield/ultimate load capacity

$P_{u\text{-}s}$, $P_{u\text{-}y}$, $P_{u\text{-}u}$ -- unstrengthened service/yield/ultimate load capacity

t_f -- Thickness of the FRP strengthening plate

t_a -- Thickness of the adhesive layer

£$_s$ -- Strain at tension steel

£$_{sp}$ -- Strain at compression steel

£$_f$ -- Strain at the centre of FRP strengthening plate

£$_c$ -- Strain at top concrete fibre

°$_s$ -- Tension steel ratio ($A_s/(bd)$)

°$_{sp}$ -- Compression steel ratio ($A_{sp}/(bd)$)

°$_f$ -- FRP strengthening material ratio ($A_f/(bd)$)

© -- Curvature

References

ACI Committee 440. (2008). *Guide for the design and construction of externally bonded FRP systems for strengthening concrete structures*. Farmington Hills, MI, USA.

ACI Committee 318. (2008). *Building code requirements for structural concrete and commentary*. Farmington Hills, MI, USA.

Achintha, P.M.M., and Burgoyne, C.J. (2008). “Fracture mechanics of plate debonding.” J. Compos. Constr. 12(4):396-404.

Bazant, Z.P., and Becq-Giraudon, E. (2002). “Statistical prediction of fracture parameters of concrete and implications for choice of testing standard.” Cem. Concr. Res. 32:529-56.

List of Figure Captions

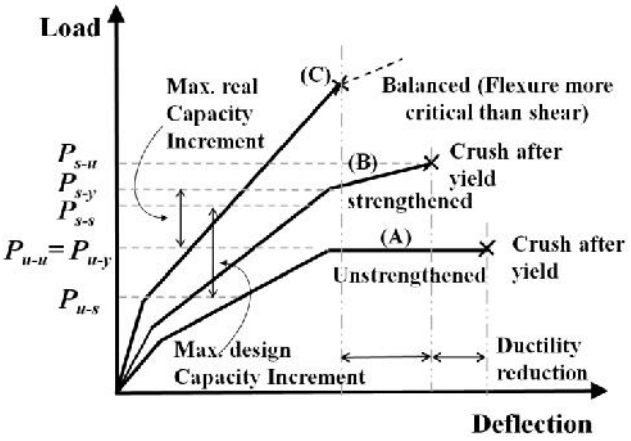

Figure 1 Considerations in FRP retrofitting design

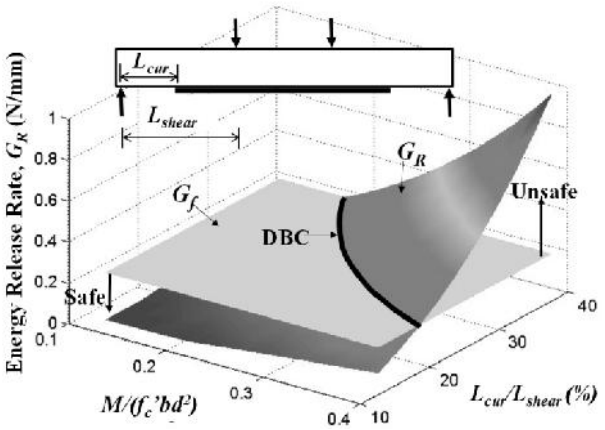

Figure 2 Determination of DBC

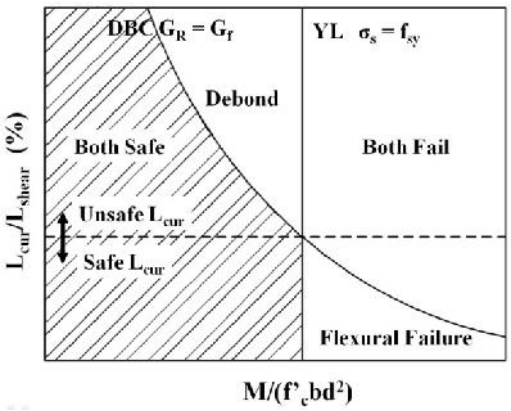

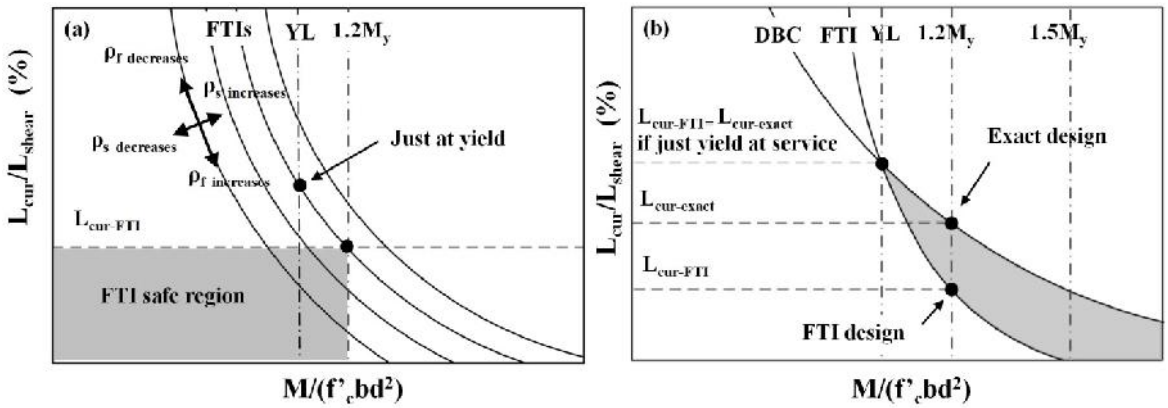

Figure 6 (a) Conceptual design chart with FTI (b) Comparison between FTI design and the exact design

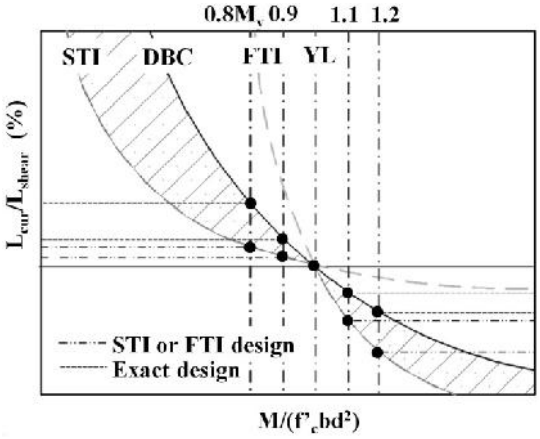

Figure 7 Comparison of the exact design, and design based on STI and FTI

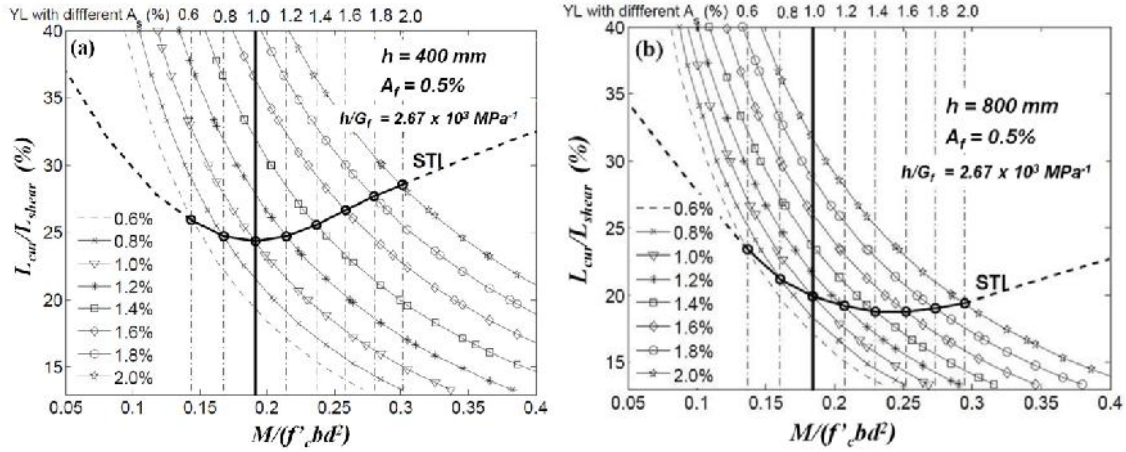

Figure 8 (a) Construction of STI for beam having h = 400 mm and G_f = 0.15N/mm (b) Construction of STI for beam having h = 800 mm and G_f = 0.15N/mm

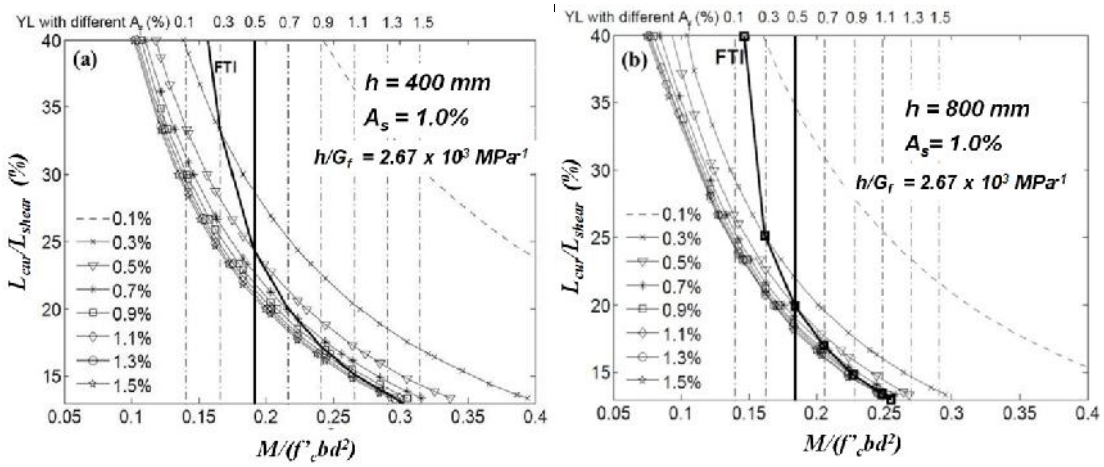

Figure 11 (a) Construction of FTI for beam having h = 400 mm and G_f = 0.15N/mm (b) Construction of FTI for beam having h = 800 mm and G_f = 0.15N/mm

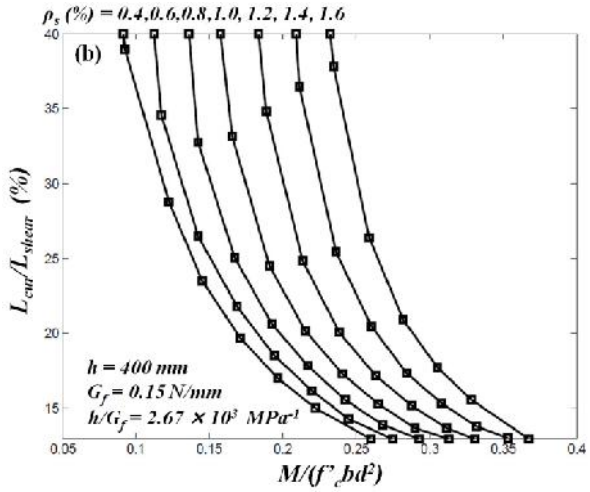

Figure 12 Numerically correct FTI for 400 mm deep beam (h/G_f = 2.67×10^3 MPa^{-1})

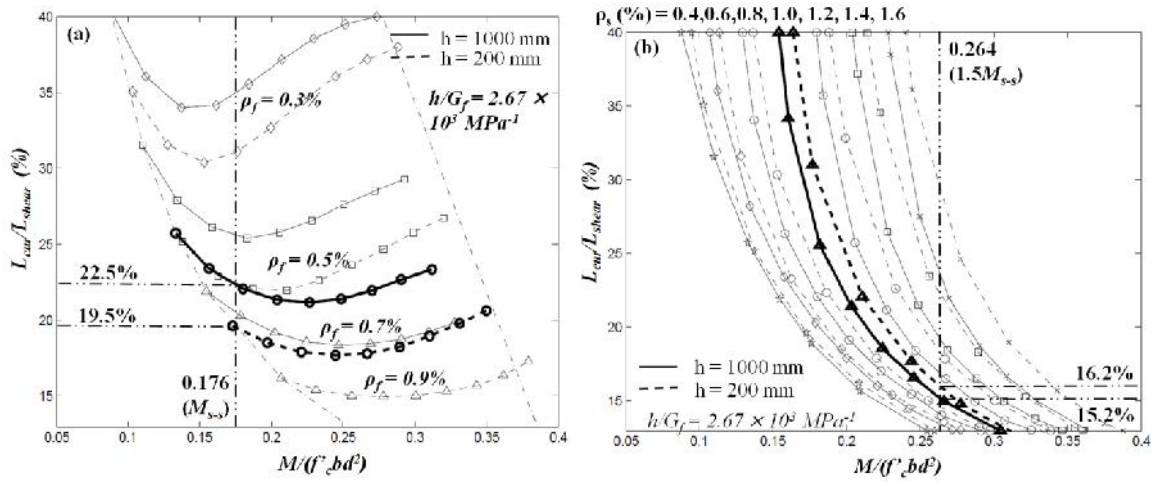

Figure 16 Determination of the $(L_{cur}/L_{shear})_{max}$ from STI and FTI band charts

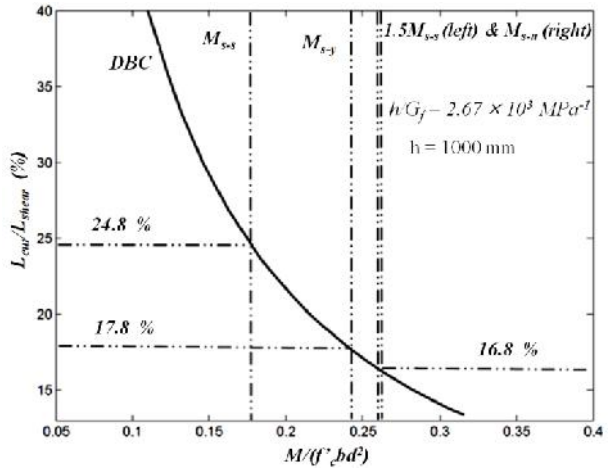

Figure 17 Debonding prevention design from DBC charts (exact design)

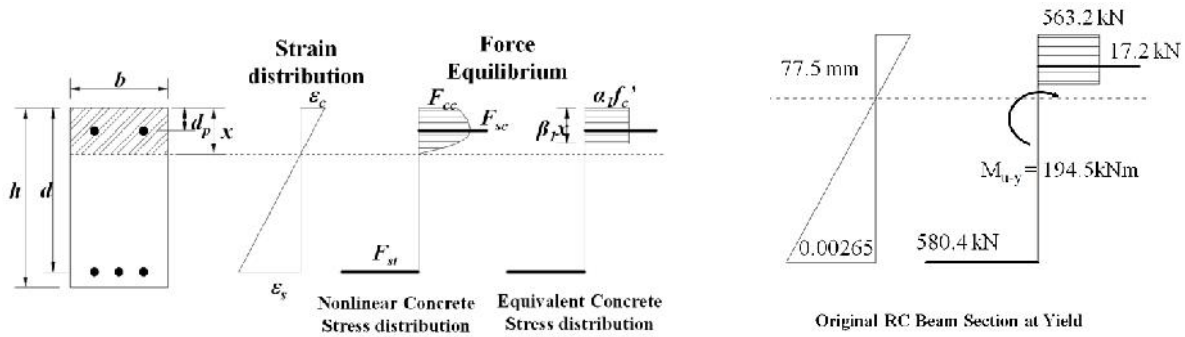

Figure 18 (a) Section analysis according to ACI; (b) Original RC beam at just yield (ultimate state)